NIH Public Access
Author Manuscript
Anal Biochem. Author manuscript; available in PMC 2012 February 13.

Published in final edited form as:
Anal Biochem. 2010 August ; 403(1-2): 88–93. doi:10.1016/j.ab.2010.04.005.

MEASUREMENT OF THE DISTRIBUTION OF AEROSOLS AMONG MOUSE LOBES BY FLUORESCENT IMAGING

Dandan Yi[1], **Andrew Price**[2], **Angela Panoskaltsis-Mortari**[2], **Amir Naqwi**[3], and **Timothy Scott Wiedmann**[1,4]

[1] Department of Pharmaceutics, University of Minnesota, Minneapolis, MN 55455

[2] Pediatric BMT and Pulmonary Medicine, University of Minnesota, Minneapolis, MN 55455

[3] Powerscope Incorporated, Minneapolis, MN 55414

Abstract

Lung samples were prepared to investigate the perturbing effects of light absorption for quantifying the fluorescence signal of aluminum phthalocyanine tetrasulfonic acid (AlPCS). Standard solutions of known concentration and depth were imaged with different exposure times and analyzed. The intensity was found to be a linear function of concentration, depth, exposure time, and area. Mice were exposed to an aerosol of AlPCS with a mass median aerodynamic diameter of 390 nm and geometric standard deviation of 1.8. Images of intact lung lobes and lung homogenates were obtained and then analyzed to allow quantifying the concentration of AlPCS among the lung lobes and trachea. For the distribution of aerosols, the results indicate that the concentration was uniform among the different lobes. Combining the quantitative analysis of the concentration with image analysis of the area/thickness, the mass deposited in each lobe was readily determined. This approach provides a quantitative means to determine the selectivity of drug delivery to mouse lower respiratory tract.

Keywords

Fluorescent imaging; lungs; aerosol; aluminum phthalocyanine tetrasulfonic acid; lung lobes

INTRODUCTION

Respiratory drug delivery is well known to provide a high localized concentration in the respiratory tract and to reduce systemic side effects in comparison to oral drug administration. However, current efforts are focused in targeting specific areas in the airways thereby maximizing drug delivery to the affected tissues. Because of the geometric complexity of the lung, assessing the mass distribution of particles within the airways in a quantitative manner is a challenging problem. The definitive methodology for humans is the combined use of positron emission tomography or gamma scintigraphy with computed tomography of x-ray (1–4). The requirement of chemical labeling and expensive

[4]To whom correspondence should be addressed: Timothy Scott Wiedmann, Ph.D., University of Minnesota, Department of Pharmaceutics, 308 Harvard St. SE, Minneapolis, MN 55455, Phone 612-624-5457, Fax 612-626-2125, wiedm001@umn.edu.

Publisher's Disclaimer: This is a PDF file of an unedited manuscript that has been accepted for publication. As a service to our customers we are providing this early version of the manuscript. The manuscript will undergo copyediting, typesetting, and review of the resulting proof before it is published in its final citable form. Please note that during the production process errors may be discovered which could affect the content, and all legal disclaimers that apply to the journal pertain.

NIH-PA Author Manuscript
NIH-PA Author Manuscript
NIH-PA Author Manuscript

NIH-PA Author Manuscript

NIH-PA Author Manuscript

NIH-PA Author Manuscript

instrumentation limits the general utility of these approaches. Moreover, the resolution is generally insufficient for rodents.

Fluorescence imaging is an attractive approach to assess the deposition of particles in the lung, since measurements can be carried out in live animals (5–8). In principle, there is a relationship between the intensity of light within a pixel, representing a two-dimensional projection of the biological sample, and the number of fluorescent molecules within the rectangular prism (7,9,10). However, both the incident excitation and the emitted fluorescent light are scattered, reflected, and absorbed by tissue, which affects the relationship between light captured by the detector and number of molecules. In addition, biological tissue also autofluoresces, which gives rise to a heterogeneous background signal.

Light absorption and autofluorescence are problems that can be corrected in a relatively straightforward manner (7,10). Light absorption is typically treated in an empirically predictable manner with the assumption that the attenuation is proportional to an exponential function of thickness. Autofluorescence can be subtracted with blank tissue, or with current instrumentation, can be essentially eliminated through judicious selection of probes that emit light at long wavelengths in the near infrared region of the spectrum (7,8). Scattering corrections are inherently more complicated, since the light from a molecule in a rectangular prism below a given pixel can be scattered such that the photons appear in a distant pixel (7,9). Thus, there is simultaneous loss/gain of the signal, which compromises the resolution of the image as well as interferes with efforts to quantify the distribution of molecules in the lung.

In this work, we have prepared lung samples to investigate the perturbing effects of absorption for quantifying the fluorescence signal of aluminum phthalocyanine tetrasulfonic acid (AlPCS). In addition, tissue was processed to allow estimation of the distribution of the fluorescent probe among the lobes of the lung.

THEORY

Consider the fluorescent image arising from irradiating a sample that contains a uniform distribution of fluorescent molecules (Figure 1). The intensity of the excitation light emitted from the source, $I_{x,o}$, is reduced in an assumed exponential manner as it passes through the tissue such that the value is $I_{x,z}$ at a distance, z, from the surface is (7)

$$I_{x,z}=I_{x,o}\exp(-\mu_x z)$$

The parameter, μ_x, is referred to as the tissue attenuation constant and has units of inverse length. Light is absorbed by the fluorescent molecules and generally the concentration is sufficiently low to assume the fraction of light absorbed is independent of depth. The fraction of light absorbed per molecule, ε, is related to the absorptivity. The fraction of the absorbed light that is emitted as fluorescence relative to that absorbed is defined as the quantum yield, Φ.

$$I_{m,o}=\Phi I_a$$

Emitted light from the molecule is also attenuated as it propagates through the tissue in a manner analogous to the excitation light, but with a distinct attenuation coefficient, μ_m.

NIH-PA Author Manuscript

NIH-PA Author Manuscript

NIH-PA Author Manuscript

$$I_{m,z}=I_{m,o}\exp(-\mu_m z)$$

In this work, we define the total attenuation coefficient, μ_t, as the sum of the excitation and emission coefficients, since they were not separated experimentally. The intensity of light in units of photons per second in unit area also falls with the distance between the source molecule and detector, since emission is taken to occur equally in all directions. This latter factor can be incorporated into a constant, if the sample is kept at a fixed distance from the detector, and the same magnification is used.

Combining these factors, the intensity of light arising from fluorescent molecules with total mass, M, located at a depth, z, is given by

$$I_{m,z}=I_{x,o}\varepsilon\Phi M\exp(-\mu_t z)$$

The total intensity is obtained by integrating over all z, which for a solution where the attenuation coefficient is taken as zero, is given as

$$I_{m,z}=I_{x,o}\varepsilon\Phi CAz$$

where the total mass of molecules is given as the product of the uniform concentration, C, area, A, and depth, z. Thus for solutions, the intensity increases linearly with concentration, area, and depth. In the presence of tissue, the intensity can be calculated as the product of the average intensity, $\langle I_{m,z}\rangle$, and the depth:

$$\begin{aligned}\langle I_{m,z}\rangle\Delta z&=\{[\int I_{x,o}\varepsilon\Phi M\exp(-\mu_t z)dz]/z\}\Delta z\\&=I_{x,o}\varepsilon\Phi CA\Delta z[1-\exp(-\mu_t z)]/\mu_t z\end{aligned}$$

Letting $\Delta z\rightarrow z$ and expanding the exponential term

$$I_{tot}=(KCA/\mu_t)[1-1+\mu_t z-\mu_t^2 z^2/2!+\cdots]$$

and taking the leading terms

$$I_{tot}=KCAz-KCA\mu_t z^2/2$$

where $K = I_{x,o}\varepsilon\Phi$, which is an instrumental constant.

Finally, it is recognized that the integrated optical density, (IOD) with units of photons as assessed from digital images, is proportional to the intensity, exposure time, T_e, and surface area, A. The surface area is measured in terms of pixels that can be calibrated to yield dimensions of length squared. Thus for solutions and tissues, respectively, the observed optical density is given the expressions below.

NIH-PA Author Manuscript

NIH-PA Author Manuscript

NIH-PA Author Manuscript

$$IOD/T_e * A * z = KC$$
$$IOD/T_e * A * z = KC - KC\mu_t z/2$$

K can be evaluated with standard solutions of known concentrations, and measuring the IOD as a function of thickness allows estimation of both the concentration and tissue attenuation coefficient of tissue samples containing a uniform concentration of fluorescent probe.

EXPERIMENTAL

Aluminum (III) phthalocyanine chloride tetrasulfonic acid was purchased from Frontier Scientific, Inc., Woburn, MA 01801. Water used in these experiments was deionized, distilled and deoxygenated. Cylinders of air were obtained from Minneapolis Oxygen Company (Minneapolis, Minnesota).

Images were taken with a CRi Maestro system (Cambridge Research & Instrumentation, Inc. (CRi 35-B Cabot Road, Woburn, MA, 01801, USA). Multispectral acquisition and analysis were used with a 649 nm excitation filter and a 700 nm long pass emission filter. Generally, images were acquired over the range of emission wavelengths of 700–800 nm in 10 nm increments. The maximum intensity was observed at 730 nm, consistent with the known properties of AlPCS (7). Images were taken of solutions that ranged in concentration from 0 to 20 μg/ml, with depths of 0.072–0.127 cm (held between microscope glass slides with spacers), and exposure times of 10–500 ms. A similar process was used to obtain images of AlPCS dispersed in lung homogenates, which were at 1:1, 1:3, or 1:5 dilution with normal saline.

The images were analyzed with Image-Pro Plus Version 6.3. First, the gray level range was set from a lower limit based on the overall intensity (30–100) and an upper limit of 4095. All the areas with intensity values falling into that range were chosen as the area of interest (AOI). The total number of pixels and integrated optical density (IOD) of the AOI were measured. The IOD represents the value of the total intensity of all pixels selected. The total intensity as determined by the sum of the intensities in the selected pixels and the area selected as number of pixels were exported to Excel for further analysis. Pixel dimensions were calibrated by imaging a ruler and determining the number of pixels in a given length.

For the aerosol exposures, female C57BL/6 mice 5–6 weeks (19–21 g) were purchased from Harlan Sprague Dawley, Inc. (Indianapolis, Indiana). The mice were allowed food and water prior to aerosol exposure. The mice were exposed to an aerosol of AlPCS that was generated with a custom-built jet nebulizer, which has an impaction dome to remove large drops, that contained a 10 mg/ml solution AlPCS and 100 mg/ml CsCl and operated at 30 psi with a compressor. The air flow rate from the nebulizer was 2 LPM. The particle size distribution was measured with a scanning mobility particle sizer (SMPS) (TSI, Minneapolis, MN). The mice were restrained by hand, and during the “nose-only” exposure of 1 min, the mice were conscious. The mice were sacrificed immediately after aerosol exposure by cervical dislocation. All procedures were carried in accordance with the approved protocol (IACUC, University of Minnesota).

The lung was severed at the carina, and the trachea and lung were removed and divided into lobes. The trachea and lobes were placed on a microscope slide and imaged. Another microscope slide was then placed on top, and the lobes were compressed to a thickness of 0.1cm, and images were obtained from the both the top and bottom perspectives. The lobes were then compressed to a thickness of 0.72 cm, and images again were obtained. Finally, the top microscope slide was removed, and the lobes were imaged again. The lobes were

NIH-PA Author Manuscript

NIH-PA Author Manuscript

NIH-PA Author Manuscript

then weighed and stored at −20 °C. After thawing, three times the weight of buffer was added to only the lobes (trachea was not included), and then the mixture was homogenized. Images of the homogenate were obtained by confining the dispersion between two microscope slides and using identical acquisition parameters as above.

To compare the intensity values among different lungs, the images were taken on the same day and with the same magnification, focus and exposure time. All images were saved in 12-bit gray scale files. The images were processed with Image-Pro plus 6.0 as described above. The tissue attenuation coefficient and concentration were estimated from the slope and intercept of a plot of the normalized intensity as a function of thickness.

RESULTS

As a prerequisite to analyzing biological samples, it is imperative to establish the sensitivity and functional dependency of the instrumental response function to area, exposure time, depth, and fluorophore concentration. It is generally accepted that the total intensity should increase linearly with area; however, this presumes that the excitation intensity is uniform. In Figure 2, an image of an AlPCS solution. As can be seen, the uniformity of the intensity is reasonably good but not perfect. The inset depicts a line cut through the image obtained with Image-Pro that reveals more clearly that the intensity is greater in the center and falls off near the perimeter.

Because of the curvature at the edge of the liquid contained within the microscope slides, the perimeter is extremely bright. For uniform samples, a straightforward correction can be applied to each pixel based on the measurement of the intensity of a uniform sample. Non-uniform samples are problematic, particularly with the instrument that was used in this study, which has four sources of excitation light in a rectangular array that illuminate the sample at an approximately 45° angle from the horizontal plane.

The second parameter is exposure time. Here again, the presumption is that the excitation rate in terms of photons reaching the fluorophore and emission rate in terms of photons reaching the detector are constant with time. This would give rise to a collection rate that is constant and therefore the intensity would be proportional to exposure time. This was confirmed by the linear plots shown in Figure 3, where the intensity normalized to pixel area is given as a function of exposure time for a 10 μg/ml solution. Due to the relatively high concentration and sensitive instrumentation, relatively short exposure times were used, and so there was little concern of photobleaching with AlPCS, which has good photostability (7). The three distinct lines shown in Figure 3 arise from images taken of three solutions with the same concentration but depths of 0.072, 0.1000, and 0.1270 cm. The slopes calculated with least squares regression were 6.11, 7.24 and 10.86/pixel*ms, which are proportionately greater with increasing depth.

The approach above was extended to an examination of different concentrations. In Figure 4, the intensity was normalized to area and depth and plotted as a function of exposure time. In this graph, each individual data point represents the mean of the results from the three different solution depths. It should be noted that at a given exposure time linear relationships were found with the intensity plotted as a function of concentration up to a value of 10 μg/ml. However at 20 μg/ml, deviation from linearity was observed (not shown) consistent with self-quenching of fluorescent molecules.

For tissues, it would be ideal to obtain an image of an intact lung lobe containing a uniform concentration fluorophore; however, this is not practically possible because of the non-uniformity of the tissue and potential change in the tissue properties giving rise to time dependence of the attenuation coefficients. As an alternative approach, a lung homogenate

NIH-PA Author Manuscript

NIH-PA Author Manuscript

NIH-PA Author Manuscript

was prepared, various amounts of AlPCS were added, and images were obtained as a function of exposure time, AlPCS concentration, depth, and homogenate concentration. The intensity was normalized to area and exposure time and plotted as a function of concentration for the three designated depths as shown in Figure 5. Analogous results to the aqueous solutions were found in terms of the linearity of the response, but as expected, the observed intensity was lower. From the reduction in intensity, the attenuation coefficient was estimated 5.5 cm^{-1} for the 1:1 dilution.

For the final set of experiments, image analysis was used to assess the deposition of aerosol particles of AlPCS in the mouse lung and distribution among the lung lobes. The geometric mean particle size and associated geometric standard deviation for the aerosol was 390 nm ± 1.81. The image of the separated lung lobes is shown in Figure 6a. It is evident that the intensity is not uniform despite the expectation that the small particle size of the aerosol would lead to relatively uniform deposition throughout the alveoli of the lungs. The curved surface coupled with the shallow depth of field cause certain areas of the image to appear out of focus. The curved surface of the intact lobes also would lead to collection of light at a specific charged-couple device (CCD) that does not correspond to the pixel directly beneath, since the refractive index difference between air and the tissue will cause the lung lobes to act as lenses. In Figure 6 panel b, the image was obtained from lobes that underwent compression and then were decompressed. While the images are similar, a close examination reveals that the detailed image intensity has been altered. It should be noted that the lungs underwent movement in removing the upper slide, so changes can not be uniquely ascribed to the compression process.

The image depicted in panel c of Figure 6 was obtained with compression of the lobes to a thickness of 0.1 cm. Comparing this image with the uncompressed lung, the clarity is improved, the lobes occupy a larger area and intensity is more uniform in that there is a loss of intensity in the bright areas that is seen with the uncompressed lobes. With further compression to 0.072 cm (Figure 6d), the area occupied increases further, and the intensity appears to lessen. Finally, images obtained from the reverse side (not shown) were distinct in terms of the intensity distribution but equal in terms of observed area.

Analysis of the intensity of each lobe as a function of thickness allowed estimation of the attenuation coefficient. The results are given in Table I where the lobes and trachea were given the following designations, L:left, RS:right superior, RM:right medial, RI:right inferior, PC:post caudal, and T:trachea. L, RS, RM, and RI had similar attenuation coefficients ranging from about 6 to values less than 11 cm^{-1}. PC and T had larger values, which is not surprising for the trachea, since it contains significantly more cartilage. The larger values of PC may be related to its irregular shape. The value itself clearly indicates the significant loss of intensity with depth, where using an attenuation coefficient of 10 cm^{-1}, the intensity will fall to 1/e at a distance of 1 mm.

In addition to the attenuation coefficient, the concentration of the deposited fluorophore was estimated for each lobe by extrapolation to zero thickness. In Table I, the mean and standard deviation for three replicates are given. For the aerosol, the concentrations in the lobes ranged from 1.8 to 2.9 μg/ml and were not significantly different by pair-wise comparisons. The trachea had a similar value of 2.37 μg/ml. The standard deviations were similar to other studies in which the total lung concentration was determined following aerosol exposure (11). Interestingly, the variability was comparable when averaged across the different lobes for the same animal (data not shown) or across the same lobe for different animals (Table I). The total concentration was determined to be 1.74 ± 0.49 μg/ml from analysis of the intensity of the homogenized lung, which is in reasonable agreement with that estimated from intact lungs.

NIH-PA Author Manuscript

NIH-PA Author Manuscript

NIH-PA Author Manuscript

With compression, the thickness of each lobe is known and the area can be estimated from the image, which allows the volume to be calculated. The results from the pixel calibration were 175.5 pixels/mm. The results are given in Figure 7 where a thickness of 0.072 cm was used. The total mean volume was 244 ± 21 mm^3, which was approximately 10 % smaller than that obtained with a compression thickness of 0.1 cm. The mass of the lung was also determined from which the density was calculated. The density ranged from 0.3 to 0.4 g/ml, which is a reasonable value for a deflated lung. With the AlPCS concentration in each lobe and the estimated volume, the mass deposited can be calculated. The values are also given in Figure 7. The distribution of mass correlates with the size of the lobe, which is consistent with equivalent inflation per mass of the lobes.

DISCUSSION

To develop respiratory drug delivery systems that are spatially selective in the deposition of drug, methods are needed to quantify the success of the delivery system. Although sophisticated methods such as PET or helical CT/gamma scintigraphy have been used, the expensive instrumentation, use of radioactivity, and specialized chemical labeling limit the broad utility. Moreover, they typically lack the needed spatial resolution for imaging small rodents. The extensive commercialization of digital cameras, image analyses, and computational software makes the use of fluorescence imaging an attractive alternative. This has been further enhanced by the introduction of molecular probes that absorb and emit light in the near infrared, which reduces the extent of tissue attenuation (7,8,12).

In developing methodology for quantifying the distribution of aerosol particles in the lung, the severe problem of tissue attenuation is difficult to overcome when using a live animal. Moreover, the two dimensional images require reconstruction to the three dimensional anatomical organ (13–15). As such, the path taken here was to excise the lungs and separate the organ into lobes. The curvature of the tissue causes distortion of the direction of the path of light secondary to the change in refractive index. This problem was solved by compressing each lobe between flat microscope slides. The thickness compression was controlled by spacers. This had the added benefit of reducing the extent of tissue attenuation. In fact, with the functional dependence of tissue attenuation assumed to be exponential, the value of the attenuation was estimated, which in turn was used to correct the observed intensity for quantifying the concentration of the probe in the lobe. Also, it readily allowed for measurement from two different perspectives, top and bottom, which further reduces the attenuation problem by dividing the thickness in half.

The tissue attenuation coefficients estimated here ranged from 6 to less than 11 cm^{-1}. These values are higher compared to those of Comsa et al (7), who examined liver and muscle using AlPCS as a point source. Since the lung is composed of alveoli that contain air, it is a much more complicated tissue from the perspective of light passage. Specifically, the heterogeneity of the refractive index due to the air/tissue interfaces can be expected to increase light scattering. The air filled alveoli introduce the possibility of multiple light reflections at the curved surfaces. These issues pose significant experimental and theoretical issues for assessing the distribution of drug within a lobe, but by limiting the analysis to intact lobes, the complications were avoided.

Homogenizing the lung lobes clearly minimized the heterogeneity of the sample as was evident from the images. The reasonable agreement between the estimated concentrations from images of intact lobes and lung homogenate indicate that the heterogeneity of the image is related to heterogeneity in the tissue attenuation. It was evident with a number of lobes that the presence of connective tissue attenuated light to a much greater extent than normal lung tissue. Thus, in excising and separating the lung lobes, it is important to remove

NIH-PA Author Manuscript

NIH-PA Author Manuscript

NIH-PA Author Manuscript

this material. Blood appeared to have a much greater attenuation coefficient than other tissue and interstitial fluid. Clotted blood is especially opaque and thereby potentially gives rise to non-uniformity unless carefully removed/avoided. On the other hand, it opens the possibility of flushing the lungs by passing saline or appropriate buffer through the lungs via the bronchial artery/right atrium of the heart.

For the distribution of aerosols, the results indicate that the concentration was uniform among the different lobes. Combining the quantitative analysis of the concentration with image analysis of the area/thickness, the mass deposited was readily determined. This approach could be combined with microscopic analysis to reveal the specific distribution of aerosols in each lobe.

Acknowledgments

Financial support was provided in part by NIH Grant HL081789 (AN). DY was supported by a fellowship from China Scholarship Council.

References

1. Martin AR, Thompson RB, Finlay WH. J Aerosol Med Pulm Drug Deliv. 2008; 21:335–42. [PubMed: 18800881]
2. Dolovich MB. Proc Am Thorac Soc. 2009; 6:477–85. [PubMed: 19687222]
3. Eberl S, Chan HK, Daviskas E. J Aerosol Med. 2006; 19:8–20. [PubMed: 16551210]
4. Weers J, Metzheiser B, Taylor G, Warren S, Meers P, Perkins WR. J Aerosol Med Pulm Drug Deliv. 2009; 22:131–8. [PubMed: 19422313]
5. Ntziachristos V, Culver JP, Rice BW. J Biomed Opt. 2008; 13:011001. [PubMed: 18456953]
6. Ntziachristos V. Proc Am Thorac Soc. 2009; 6:416–8. [PubMed: 19687213]
7. Comsa DC, Farrell TJ, Patterson MS. Phys Med Biol. 2008; 53:5797–814. [PubMed: 18827315]
8. Adams KE, Ke S, Kwon S, Liang F, Fan Z, Lu Y, Hirschi K, Mawad ME, Barry MA, Sevick-Muraca EM. J Biomed Opt. 2007; 12:024017. [PubMed: 17477732]
9. Mohajerani P, Adibi A, Kempner J, Yared W. J Biomed Opt. 2009; 14:034021. [PubMed: 19566314]
10. Chen TW, Lin BJ, Brunner E, Schild D. Biophys J. 2006; 90:2534–47. [PubMed: 16387783]
11. Liao X, Liang W, Wiedmann T, Wattenberg L, Dahl A. Exp Lung Res. 2004; 30:755–69. [PubMed: 15700551]
12. Kovar JL, Simpson MA, Schutz-Geschwender A, Olive DM. Anal Biochem. 2007; 367:1–12. [PubMed: 17521598]
13. Xia Z, Huang X, Zhou X, Sun Y, Ntziachristos V, Wong ST. IEEE Trans Inf Technol Biomed. 2008; 12:569–78. [PubMed: 18779071]
14. Rostami AA. Inhal Toxicol. 2009; 21:262–90. [PubMed: 19235608]
15. Jaafar-Maalej C, Andrieu V, Elaissari A, Fessi H. Expert Opin Drug Deliv. 2009; 6:941–59. [PubMed: 19637979]

NIH-PA Author Manuscript

NIH-PA Author Manuscript

NIH-PA Author Manuscript

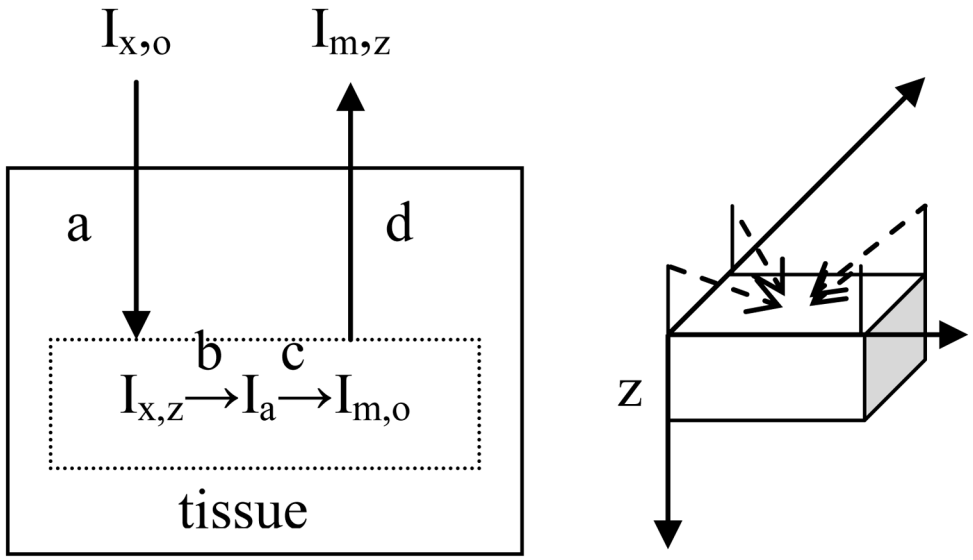

Figure 1.

Schematic diagram of processes affecting the light intensity (a) attenuation of excitation light, (b) light absorption by fluorophore, (c) fluorescent light emission, and (d) attenuation of emitted light and relationship to the geometry of the image. The axis system used is shown to the right with z taken as a measure of depth starting from the surface of the tissue. The four dotted lines indicate the diagonal arrangement of the four excitation light sources positioned at a 45° angle to the plane of the surface of the sample.

NIH-PA Author Manuscript

NIH-PA Author Manuscript

NIH-PA Author Manuscript

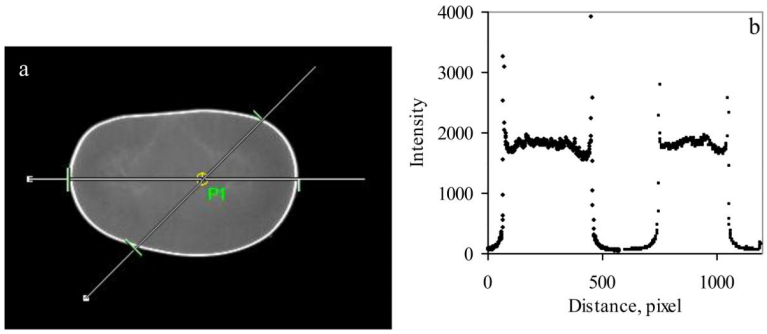

Figure 2.

(a) Image of 10 ug/ml AlPCS solution contained between two microscope slides with point P1 indicating the center of the four sources of light and the lines indicating the line cuts along which the intensity was measured using Image-Pro software with the values given in plot (b) where the intensity of the horizontal line (left) is given as a function of pixel number and a similar plot is given for the 45° line (right) where the pixel number corresponds to a greater length by the square root of two.

NIH-PA Author Manuscript

NIH-PA Author Manuscript

NIH-PA Author Manuscript

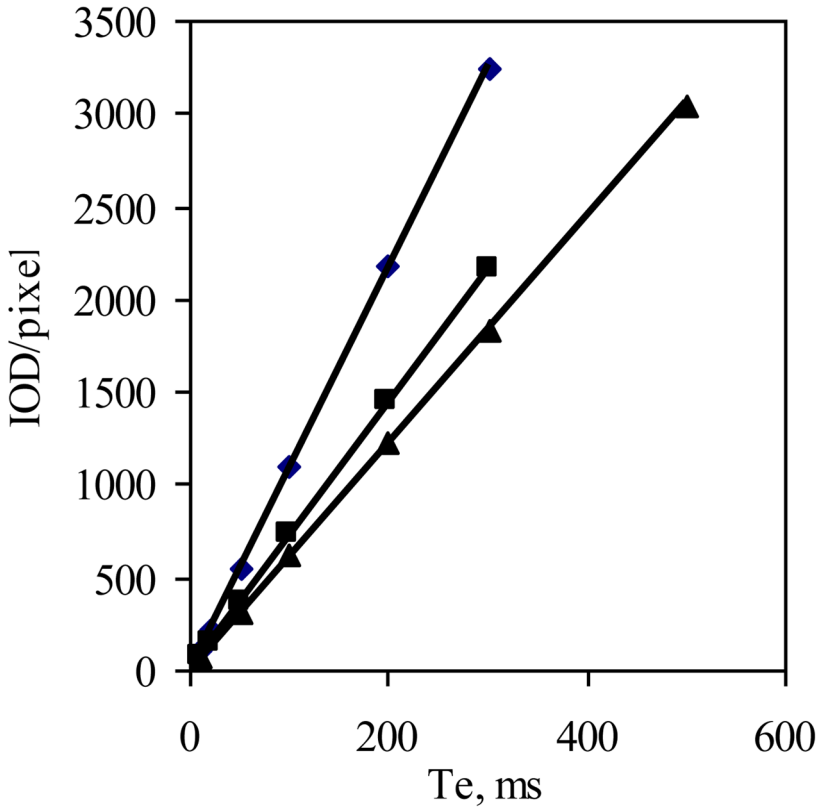

Figure 3.
Images of a 5 μg/ml solution of AlPCS where obtained as a function of exposure time constrained to a specified depth, and the integrated intensity normalized to the number of pixels is plotted as a function of exposure time for three depths of (▲) 0.072, (■) 0.1, and (◆) 0.127 cm (n=3, where the SD is smaller than the size of the point).

NIH-PA Author Manuscript

NIH-PA Author Manuscript

NIH-PA Author Manuscript

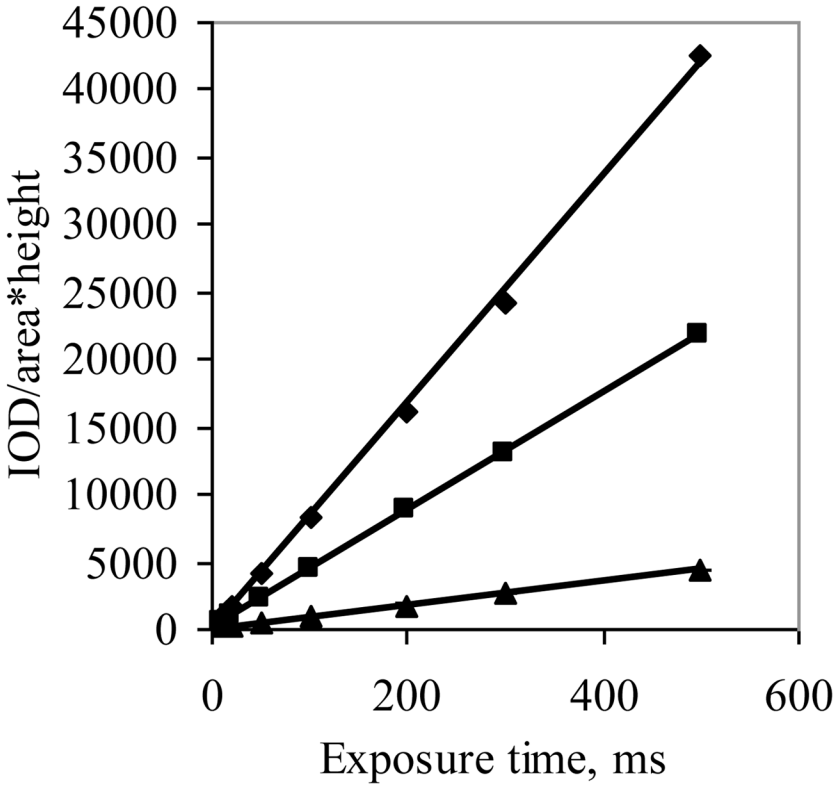

Figure 4.
Images of three different solutions of AlPCS with concentrations of (▲) 2.5, (■) 5, and (◆) 10 μg/ml were obtained as a function of exposure time, and the integrated intensity normalized to the number of pixels and solution height in centimeters is plotted as a function of exposure time (n=3, where the SD is smaller than the size of the point).

NIH-PA Author Manuscript

NIH-PA Author Manuscript

NIH-PA Author Manuscript

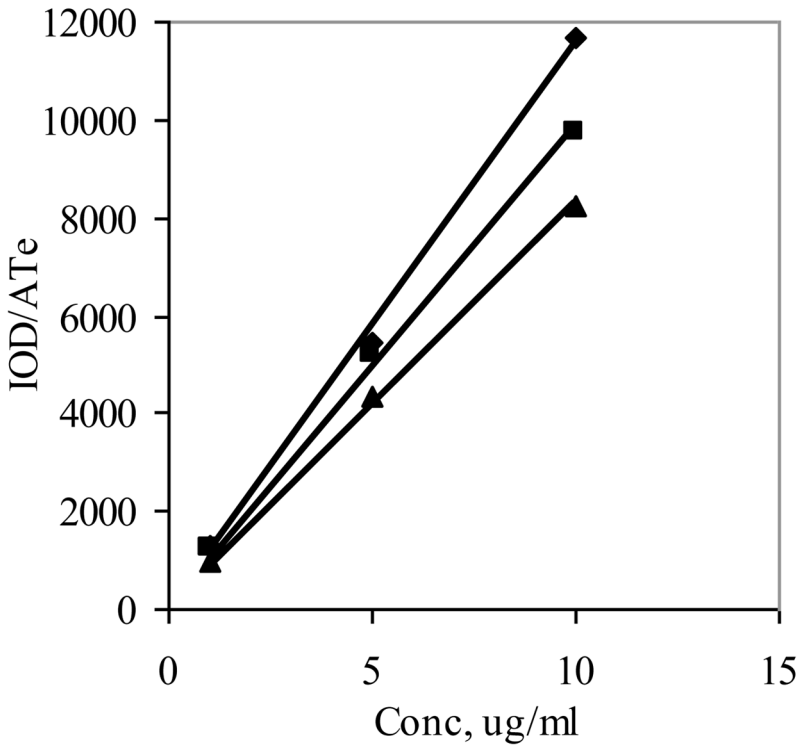

Figure 5.
Images of the AlPCS in lung homogenate:buffer dispersion (1:1) with depths of (▲) 0.072, (■) 0.1, and (◆) 0.127 cm were obtained as a function of concentration and the integrated intensity normalized to the number of pixels, A, and exposure time, Te, is plotted as a function of concentration (n=3, where the SD is smaller than the size of the point).

NIH-PA Author Manuscript

NIH-PA Author Manuscript

NIH-PA Author Manuscript

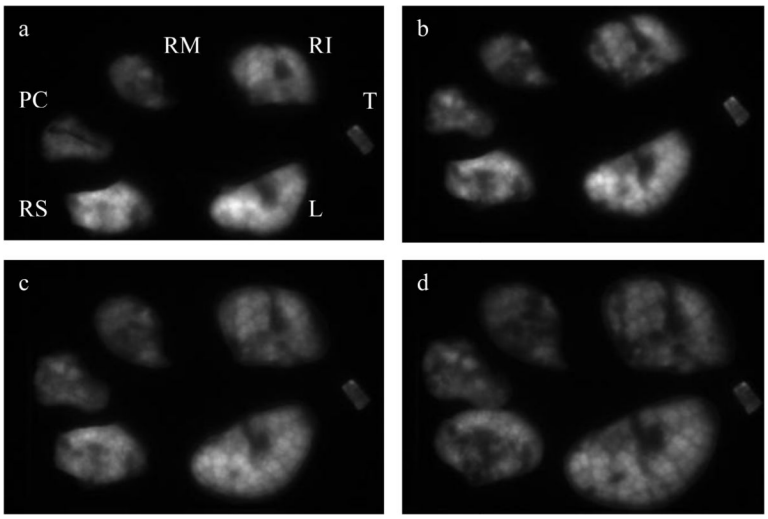

Figure 6.

Mice were exposed to an aerosol of AlPCS and the above figure of the lung lobes were obtained by converting the raw images to a 12 bit gray scale and increasing the contrast of each image in an identical manner where (a) initial excised lobes, (b) lobes after compression, (c) lobes compressed to a thickness of 0.1 cm, (d) compressed to a thickness of 0.072 cm. The lobe designations are L:left, RS:right superior, RM:right medial, RI:right inferior, PC:post caudal, and T:trachea

NIH-PA Author Manuscript

NIH-PA Author Manuscript

NIH-PA Author Manuscript

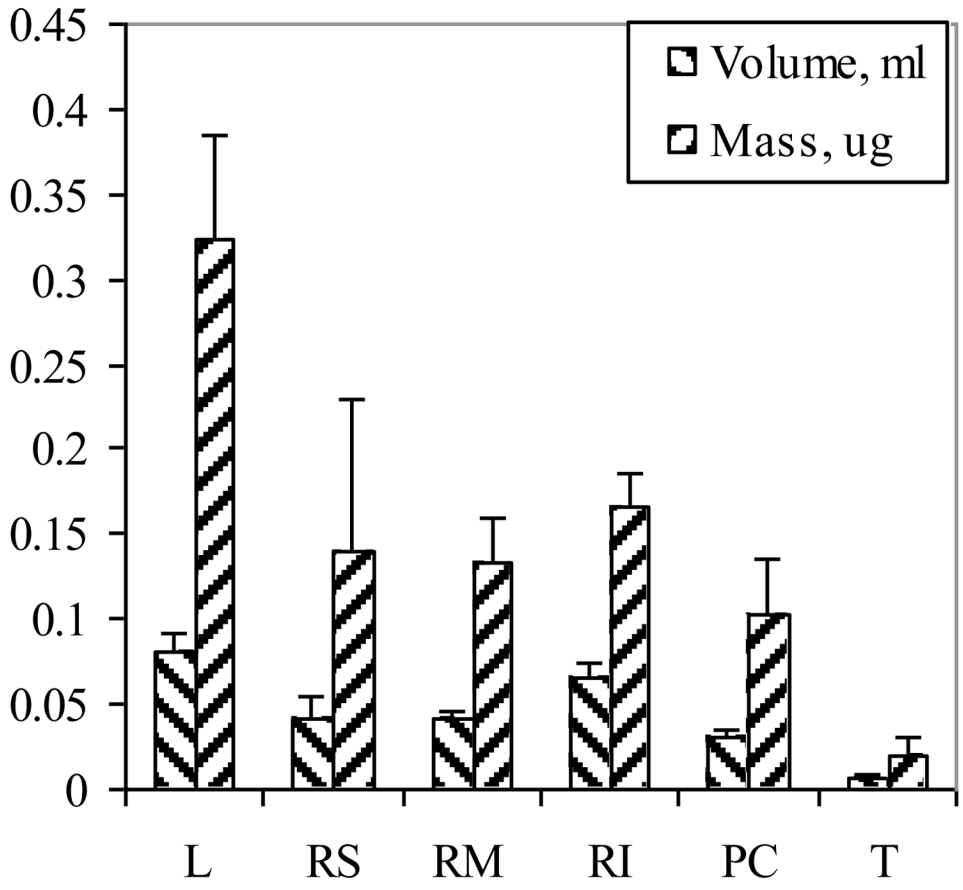

Figure 7.
Lung lobe volumes were calculated from the product of the area and depth of images obtained following aerosol exposure, and the mass of AlPCS was determined in each lobe from the product of the concentration estimated from the extrapolated value of the intensity at zero depth and the lobe volume (n=3, ± SD). The lobe designations are L:left, RS:right superior, RM:right medial, RI:right inferior, PC:post caudal, and T:trachea.

NIH-PA Author Manuscript
NIH-PA Author Manuscript
NIH-PA Author Manuscript

Table I

Mice were exposed to an aerosol of AlPCS and the lungs were excised, compressed to two different thicknesses, and imaged. ImagePro was used to determined the intensity at each thickness and the attenuation coefficients and concentration of AlPCS (mean ± SD, n=3) were calculated as described in the experimental section.

	L	RS	RM	RI	PC	T
Attenuation coefficient, cm^{-1}	6.3 ± 1.2	8.3 ± 1.4	9.1 ± 1.2	5.5 ± 1.6	10.8 ± 0.5	10.7 ± 1.9
Concentration, μg/g	2.89 ± 0.40	2.3 ± 1.1	2.40 ± 0.39	1.80 ± 0.08	2.75 ± 0.59	2.37 ± 0.96

Anal Biochem. Author manuscript; available in PMC 2012 February 13.